ACS Chemical Neuroscience

Research Article

pubs.acs.org/chemneuro

Amyloid Plaque-Associated Oxidative Degradation of Uniformly Radiolabeled Arachidonic Acid

Ran Furman,[†] Ian V. J. Murray,[‡,§] Hayley E. Schall,[‡] Qiwei Liu,[†] Yonatan Ghiwot,[‡] and Paul H. Axelsen*[,†]

[†]Department of Pharmacology, The University of Pennsylvania, Philadelphia, Pennsylvania 19104, United States

[‡]Department of Neuroscience and Experimental Therapeutics, Texas A & M University, College Station, Texas 77807, United States

[§]Department of Physiology and Neuroscience, St. George's University, St. George's, Grenada

Supporting Information

ABSTRACT: Oxidative stress is a frequently observed feature of Alzheimer's disease, but its pathological significance is not understood. To explore the relationship between oxidative stress and amyloid plaques, uniformly radiolabeled arachidonate was introduced into transgenic mouse models of Alzheimer's disease via intracerebroventricular injection. Uniform labeling with carbon-14 is used here for the first time, and made possible meaningful quantification of arachidonate oxidative degradation products. The injected arachidonate entered a fatty acid pool that was subject to oxidative degradation in both transgenic and wild-type animals. However, the extent of its degradation was markedly greater in the hippocampus of transgenic animals where amyloid plaques were abundant. In human Alzheimer's brain, plaque-associated proteins were post-translationally modified by hydroxynonenal, a well-known oxidative degradation product of arachidonate. These results suggest that several recurring themes in Alzheimer's pathogenesis, amyloid β proteins, transition metal ions, oxidative stress, and apolipoprotein isoforms, may be involved in a common mechanism that has the potential to explain both neuronal loss and fibril formation in this disease.

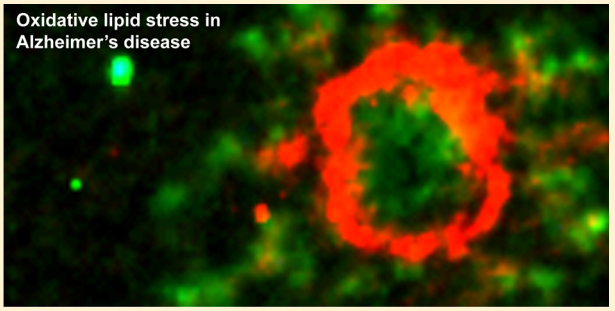

KEYWORDS: *Oxidative stress, polyunsaturated fatty acids, Alzheimer's disease*

Oxidative stress is a heterogeneous network of chemical reactions that are generally deleterious to cells. These reactions are commonly observed in Alzheimer's disease (AD),[1] although their precise role in its pathogenesis is not understood. One possible role is suggested by the in vitro observation that the amyloid beta (Aβ) peptides that aggregate into fibrils and form neuritic plaques in AD, can also form high-affinity complexes with metal ions such as copper, undergo redox cycling, and generate hydroxyl radicals ($^{\bullet}$OH).[2−7] Polyunsaturated fatty acyl (PUFA) chains, such as arachidonic (ARA) and docosahexaenoic (DHA) acids, are abundant in brain and especially vulnerable to $^{\bullet}$OH attack,[8,9] which yields well-known hydroxylated and hydroperoxylated addition products, as well as hydroxyalkenals, oxoalkenals, malondialdehyde, and acrolein as degradation products.[10−14] Several of these products, including acrolein and 4-hydroxy-2-nonenal (HNE), are known to be elevated in AD[15−17] and have been implicated in mediating the neurotoxicity of Aβ peptides,[18−21] possibly through the formation of protein adducts.[22−27] Therefore, oxidative stress at synaptic terminals, where Aβ peptides and free copper ions are especially abundant, may be responsible for creating the neurotoxins that lead to synaptic and neuronal loss.[28−38]

In addition to its neurotoxicity, HNE dramatically accelerates fibril formation by Aβ peptides.[39,40] The mechanism of this acceleration appears to depend on the presence of a membrane surface, possibly as a nucleation site for membrane-associated HNE-modified Aβ peptides.[41,42] In this context, it is noteworthy that HNE, which is a product of omega-6 PUFA oxidation, promotes both membrane association and Aβ fibril formation, while 4-hydroxy-2-hexenal (HHE), an omega-3-derived analogue of HNE, has neither effect.[43] Therefore, the tendency for oxidative stress to induce Aβ fibril formation may depend on the relative availability of omega-3 versus omega-6 substrates.

The current study was performed to address three critical questions about oxidative stress and PUFAs in AD. The first question is whether exogenously introduced ARA reaches the pool of fatty acids that are subject to the kind of oxidative stress that is elevated in mouse models of AD. This question is important because it implies that radiolabeled ARA may be used to quantify and track the fate of the whole spectrum of ARA oxidation products, not merely representative or relatively unreactive products.

The second critical question is whether oxidative ARA degradation is specifically increased in portions of the brain where the histopathological lesions of AD are well developed.

Received: December 2, 2015
Accepted: January 22, 2016
Published: January 22, 2016

DOI: 10.1021/acschemneuro.5b00316
ACS Chem. Neurosci. 2016, 7, 367−377

Prior studies have observed that an increase in the production of oxidative stress markers precedes the development of AD histopathology in mouse models,[44,45] but they have not shown that their production is plaque-associated.

The third critical question is whether fibrillogenic oxidative ARA degradation products, previously demonstrated only in mice, may also be demonstrated in human AD. HNE has been shown to form pyrrole adducts with the lysine residues of various proteins, in particular the tau proteins that form neurofibrillary tangles in mouse models of AD.[22−24] However, HNE acting on Aβ peptides results in histidine modification, and this modification is potently fibrillogenic.[39,40,43,46] Immunohistochemical evidence of plaque-associated HNE in human, mouse,[47] and dog brain[48] has been described. However, this evidence was obtained with antibodies having broad reactivity. Antibodies specific for the HNE-histidine modifications that result from the action of HNE on Aβ peptides have demonstrated their colocalization with amyloid plaques in mice.[49] The corresponding demonstration in human tissue is important to support the relevance of these findings in mouse models to human AD.

In the experiments described below, the conversion of exogenously introduced arachidonic acid to polar metabolites was markedly increased only in the hippocampus of mice where Aβ plaques are well developed, and HNE-histidine adducts colocated with amyloid plaques in human AD brain. These results suggest that ARA is oxidatively degraded in the vicinity of amyloid plaques, yielding products that are both neurotoxic and fibrillogenic.

RESULTS

The Rate of [1-^{14}C]-ARA Conversion in WT Mouse Brain. [1-^{14}C]-ARA was introduced by intracerebroventricular (ICV) injection into 22 month old C57BL/6J (WT) mice that were then euthanized 1−6 days later. Lipids were extracted from the brain tissue, saponified to liberate ARA and its metabolites, and then fractionated by HPLC. Overall, approximately 9% of the injected ^{14}C activity was recovered from the brain, similar to previously reported studies,[50−52] and that percentage did not decline significantly over the 6 day incubations. Specific radioactivity in the cerebellum (DPM/mg wet brain tissue) was higher than that of whole brain after 1 day, but declined by 3 and 6 days (Figure 1A). Specific radioactivity in the hippocampus increased compared to whole brain between 1 and 3 days, but then declined by day 6. The percentage of recovered radioactivity found in the upper, hydrophilic, phase of a Bligh−Dyer (BD) lipid extract did not change significantly over 6 days (Figure 1B). However, the percentage of recovered activity found in the saponified, hydrophobic lower phase of the BD extract that eluted in fraction V from the reverse phase column, presumably unmodified ARA, decreased over time in both the cerebellum and hippocampus (Figure 1C).

These results indicate that ARA, delivered by ICV injection into WT mice, was extensively metabolized within 1 day, yielding compounds that partition into both upper and lower phases of a BD extract. Chromatographic analysis indicates that 10−20% of the injected ARA was converted to polar products within 1 day, and conversion continued at that rate for several days. However, the presence of radiolabel in only the carboxyl position did not permit following the fate of ARA to oxidation products that did not retain the labeled C_1 carbon. Therefore,

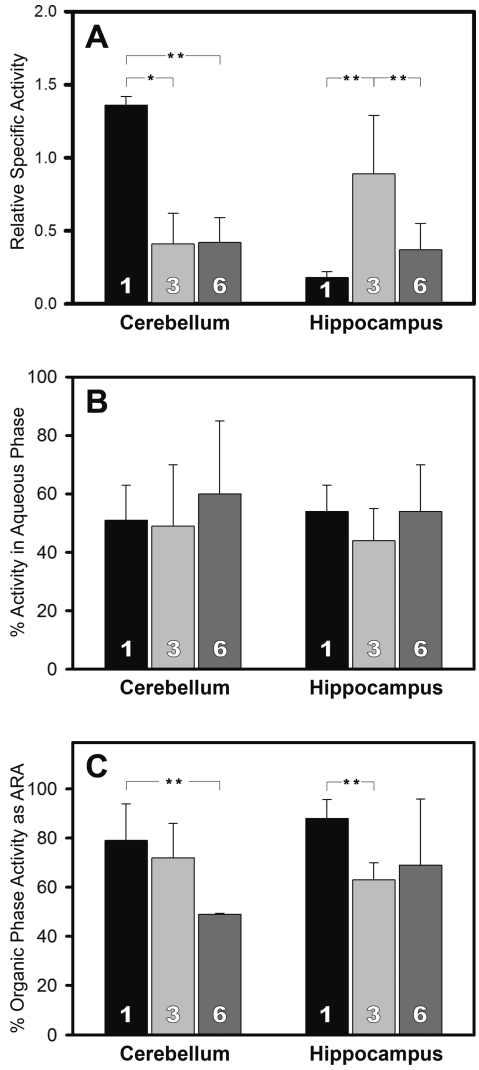

Figure 1. Fate of [1-^{14}C]-ARA in WT mouse brain. (A) Specific radioactivity (DPM/gram tissue wet mass) of cerebellum and hippocampus, divided by the whole brain specific radioactivity, to yield "relative specific radioactivity". (B) Percentage of total brain radioactivity that partitioned to the middle and upper (hydrophilic) phases of a Bligh−Dyer extract. There were no significant differences among these results. (C) The percentage radioactivity that eluted with the retention time characteristic of ARA. Error bars indicate standard deviations, and white numerals on the bars indicate the number of days after ICV injection. *Indicates a difference with $0.01 < P < 0.05$. **Indicates a difference with $P < 0.01$. P values were determined by t test.

we obtained uniformly labeled [U-^{14}C]-ARA for subsequent experiments.

The Fate of [U-^{14}C]-ARA in WT and TG-J20 Mouse Brain. [U-^{14}C]-ARA was introduced by ICV injection to 16-month-old WT and TG-J20 mice that were then euthanized after 3 days. TG-J20 begin developing plaques at the age of 10 months, so these mice had well-developed plaques (data not shown). No significant differences were observed in the relative specific radioactivity of cerebellum and hippocampus in WT and J20 mice (Figure 2A). Similarly, there was no significant difference in the percentage of radioactivity that partitioned into the upper BD phase from cerebellum and hippocampus between WT and J20 mice (Figure 2B).

DOI: 10.1021/acschemneuro.5b00316
ACS Chem. Neurosci. 2016, 7, 367−377

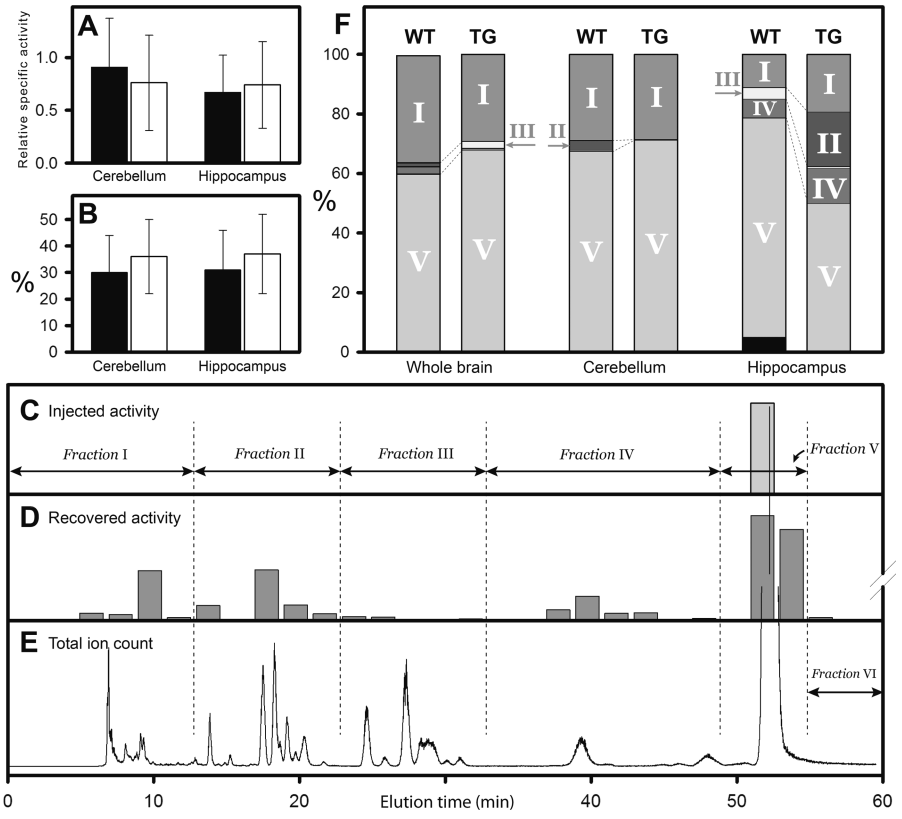

Figure 2. Fate of [U-^{14}C]-ARA in WT and J20 TG mouse brain. (A) The relative specific radioactivity in the cerebellum and hippocampus of WT (n = 16) and TG (n = 20). There were no significant differences. (B) Percentage of total brain radioactivity that partitioned to the middle and upper (hydrophilic) phases of a Bligh−Dyer extract. There were no significant differences. (C) Activity in 2 min HPLC fractions from the stock [U-^{14}C]-ARA solution used for ICV injection, subjected to extraction and saponification as for tissue samples. Arbitrary vertical scale. Intervals mark the six pooled fractions into which the 2 min fractions were groups for analysis. Characteristic compounds eluting into these fractions are listed in Table 1. (D) Representative activity in 2 min HPLC fractions from the hippocampus of a TG mouse. (E) Total ion chromatogram for MRM transitions of known oxidized ARA derivatives. (F) Averaged percentages of total recovered activity in the six pooled fractions for whole brain (n = 6WT/7TG), cerebellum (n = 9WT/8TG), and hippocampus (n = 9TG/8WT).

Materials in the lower, hydrophobic, phase of the BD extract were saponified and fractionated by reversed-phase HPLC. Samples of the [U-^{14}C]-ARA stock (the material used for ICV injections) were also processed in the same manner (i.e., extracted and saponified), and were found to elute almost entirely in fraction V. This result indicates that the [U-^{14}C]-ARA was chemically intact at the time of injection, and was not oxidatively degraded prior to injection or during tissue processing (Figure 2C). Extracts of hippocampus, in contrast, invariably contained significant amounts of activity that eluted into fractions I, II, and IV (Figure 2D). Compounds eluting into the various fractions were identified by negative ion multiple-reaction monitoring tandem mass spectrometry (Figure 2E) and are listed in Table 1. It should be noted that the compounds in fractions II and III do not arise from normal enzymatic activity operating on ARA, but rather from direct free-radical attack.

The distribution of [U-^{14}C]-ARA-derived activity across the six fractions was similar in whole brain and cerebellum, and in WT and J20 mice, with nearly all activity found in fractions I and V. Similarly, in hippocampus from WT mice most of the activity was found in fractions I and V, with some residual activity in fractions III, IV, and VI. In contrast, striking differences were observed in the hippocampus of J20 mice, where [U-^{14}C]-ARA-derived activity in fractions I, II, and IV was sharply increased compared to WT at the expense of fractions V and VI These results suggest that ARA metabolism in the hippocampus differs fundamentally from that of other brain regions, and that its oxidative degradation is markedly accelerated in J20 mice.

Table 1. Characteristic Compounds Eluting in Each of the Six Pooled HPLC Fractions

fraction	time (min)	species
I	0−12	>2 added oxygens, e.g., isoprostanes
II	12−22	1−2 added highly polar oxygens, e.g., hydroxyeicosatetraenoic acids, and hydroperoxyicosatetraenoic acids
III	22−32	1−2 added weakly polar oxygens, epoxyeicosatetraenoic acids
IV	32−48	other PUFAs, e.g., eicosapentaenoic acid and docosapentaenoic acid
V	48−54	ARA
VI	54−60	unknown

The Fate of [U-^{14}C]-ARA in WT and TG-5xFAD Mouse Brain. 5xFAD mice were obtained to examine the metabolism of ARA in a mouse model that exhibits plaque development and neuronal loss at a much younger age (3−6 months), and on a different genetic background (the WT mice to which 5xFAD animals were compared represent a different strain than the WT mice compared to J20 animals above). The relative specific radioactivity of cerebellar tissue 3 days after [U-^{14}C]-

DOI: 10.1021/acschemneuro.5b00316
ACS Chem. Neurosci. 2016, 7, 367−377

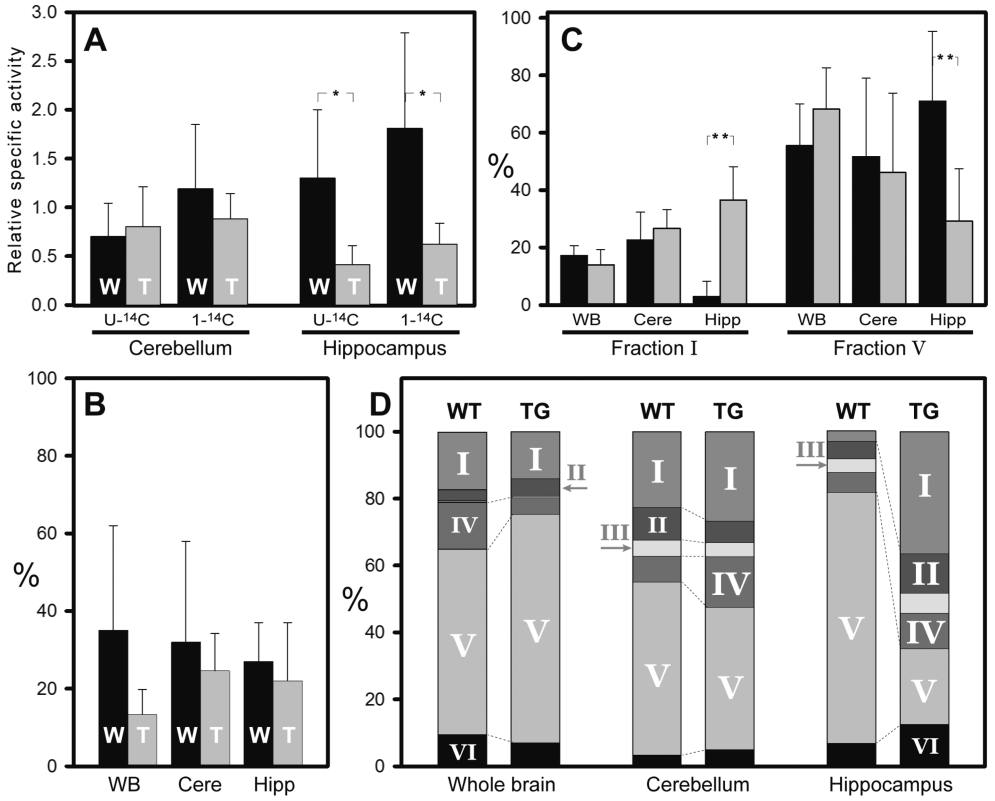

Figure 3. Fate of [U-^{14}C]-ARA and [1-^{14}C]-ARA in WT and 5xFAD TG mouse brain. (A) Relative specific radioactivity in the cerebellum and hippocampus of WT (n = 10) and TG (n = 7) mice injected with [U-^{14}C]-ARA, and WT (n = 4) and TG (n = 4) injected with [1-^{14}C]-ARA. (B) Percentage of total brain radioactivity in WT and 5xFAD mouse brain that partitioned to the middle and upper (hydrophilic) phases of a Bligh−Dyer extract. There were no significant differences. (C) Activity in pooled fractions I and V from WT (black) and 5xFAD (gray) mice as a percentage of total recovered radioactivity. The data represents an average percentage of total recovered activity from whole brain (n = 7WT/8TG), cerebellum (n = 7WT/7TG), and hippocampus (n = 8WT/5TG). (D) Averaged percentages of total recovered activity in the six pooled fractions for whole brain, cerebellum, and hippocampus (animal numbers as in panel C). *Indicates a difference with 0.01< P < 0.05. **Indicates a difference with P < 0.01. P values were determined by t test.

ARA injection was similar in J20 and 5xFAD, but it was markedly lower in the hippocampus of 5xFAD mice (Figure 3A, compare to Figure 2A). The fraction of radioactivity in the upper and middle phases of the BD extract was also similar between the two TG strains.

The relative specific radioactivity of cerebellar tissue was similar in WT and 5xFAD mice, but it was markedly lower in the hippocampus of 5xFAD compared to WT control (Figure 3A). Results with [U-^{14}C]-ARA and [1-^{14}C]-ARA were similar, indicating that the reduction in specific radioactivity of the hippocampus in 5xFAD mice was not due to a loss of $^{14}C_1$ from ARA. There were no statistically significant differences in the fraction of radioactivity in the upper and middle phases of the BD extract between WT and 5xFAD mice (Figure 3B).

As described above for J20 mice, radiolabeled compounds in the lower phases of BD extracts from 5xFAD and WT mice were saponified and fractionated by HPLC. The distribution of [U-^{14}C]-ARA-derived activity across the six fractions was more complex in 5xFAD than in J20 (Figure 3D, compare to Figure 2F), with measurable amounts of activity recovered in fractions II, IV, VI from all brain regions in both WT and 5xFAD strains. However, statistically significant differences between 5xFAD and WT were only observed in the hippocampus. There was a marked reduction in fraction V activity (i.e., unmodified ARA) in 5xFAD compared to WT, with a corresponding increase in fraction I activity (Figure 3C). There is a positive correlation between the percentage of radioactivity in fraction V and the relative specific radioactivity in the hippocampus but not in the cerebellum (Figure 5), implying that elevated ARA degradation results in lower levels of U-^{14}C-ARA in the hippocampus. Taken together, results from 5xFAD mice agree with results from J20 mice, namely that the conversion of ARA to polar degradation products is markedly accelerated in the hippocampus of TG mice compared to WT controls.

Evidence for Plaque-Associated ARA Degradation in Human AD Brain. The rise in fraction I activity associated with a fall in fraction V activity suggests that the conversion of ARA into polar oxidative degradation products is accelerated in the hippocampus of TG mice. However, the analysis employed in this study cannot identify specific oxidation products. HNE, for example, either reacts with proteins or is destroyed during saponification. Therefore, immunohistochemical methods aimed at identifying specific oxidation products in tissues were employed. Prior studies of HNE distribution in human, mouse,[47] and dog[48] brain were performed with antibodies to HNE-treated KLH protein that bind to HNE and various HNE-adducts. The use of antibodies specific for HNE-modified His residues has demonstrated HNE-His adducts in the immediate vicinity of Aβ plaques,[49] but only in a mouse model.

In Figure 4, the association of HNE-modified His residues and amyloid plaques is demonstrated in postmortem human brain. There were no HNE-His adducts detected apart from plaques, and none detected in non-AD controls. Anti-HNE-His binding did not precisely coincide with anti-Aβ antibody

DOI: 10.1021/acschemneuro.5b00316
ACS Chem. Neurosci. 2016, 7, 367−377

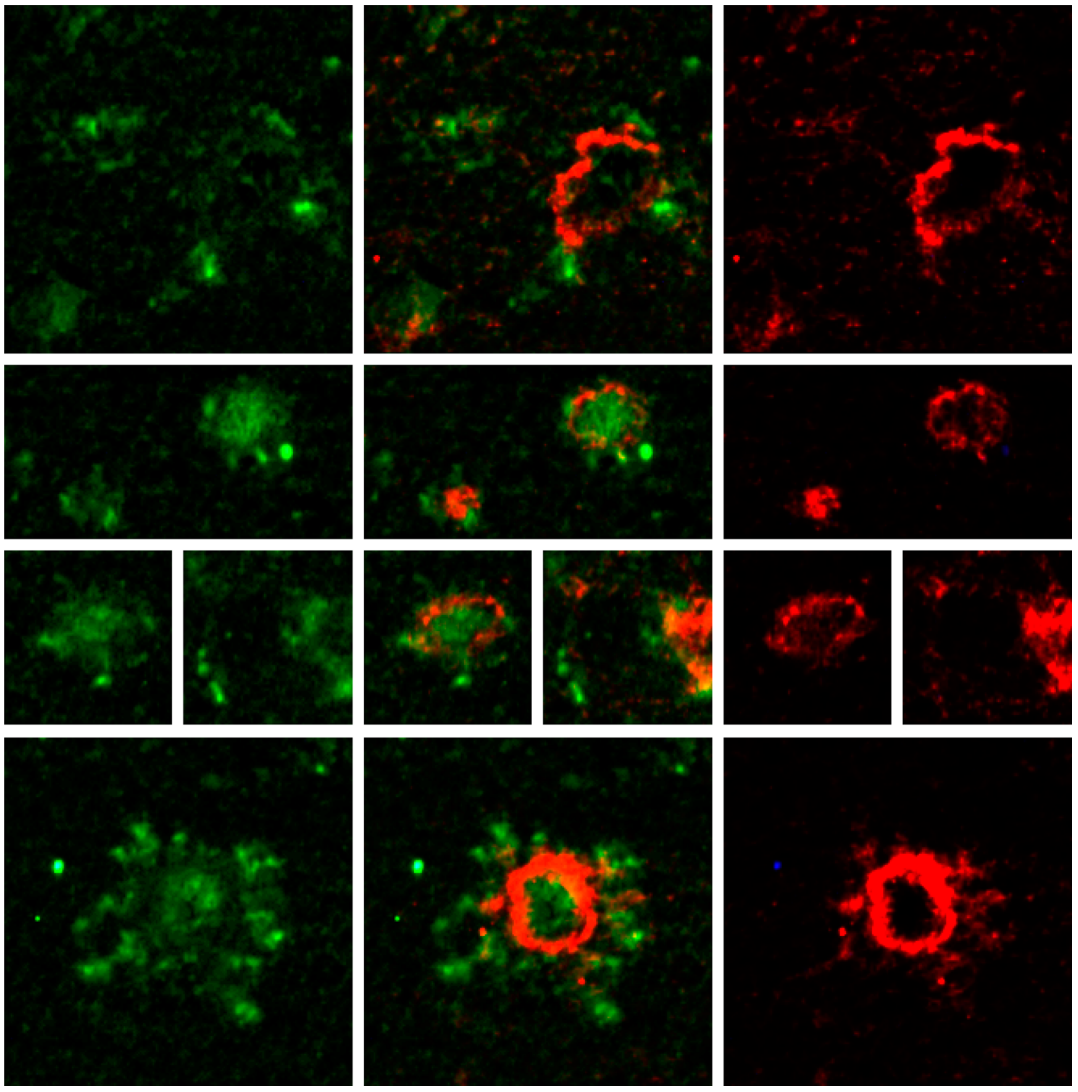

Figure 4. Immunofluorescence. The brain from the temporal cortex of an 89 year old woman with Braak stage V/VI Alzheimer's disease at autopsy after a 9 h postmortem interval was stained with anti-Aβ (left) or anti-HNE-His (right). The center images are merged left and right images. Large square images are 50 × 50 μm; other images to same scale.

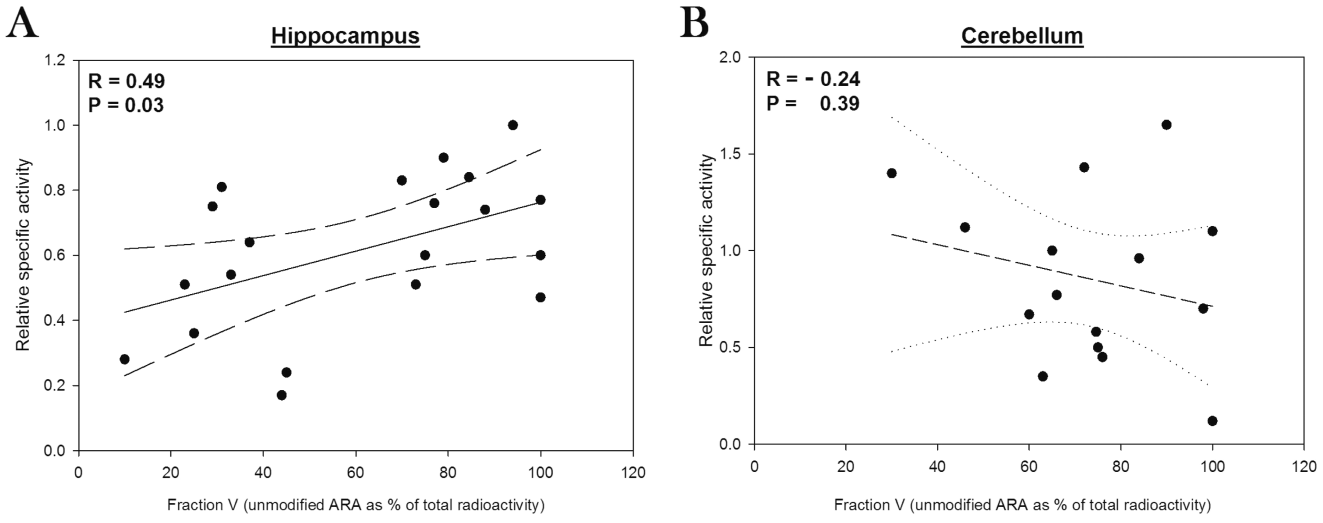

Figure 5. Correlation analysis. The fraction of total radioactivity that elutes as unmodified ARA (fraction V) is shown versus relative specific activity for (A) hippocampus and (B) cerebellum. Data for WT, TG, J20 and 5xFAD mice are aggregated.

DOI: 10.1021/acschemneuro.5b00316
ACS Chem. Neurosci. 2016, 7, 367−377

binding, but instead appeared to form a halo around each plaque. The lack of anti-HNE-His binding to amyloid plaque may have a trivial explanation, but one possible nontrivial explanation is that HNE production is due to a nonfibrillar form of Aβ peptide on the periphery of a plaque that is in equilibrium with fibrillar Aβ peptide comprising the plaque.

In summary, this result indicates that the ARA-derived degradation products capable of inducing fibril formation, and previously found in the vicinity of amyloid plaque in TG mouse, are also found in human AD.

DISCUSSION

These results demonstrate that when ARA is introduced by ICV injection, it reaches regions of the TG mouse brain where accelerated oxidative degradation is occurring and where Aβ plaques are abundant. Coupled with an immunohistochemical demonstration in human brain that ARA degradation products form protein adducts in the immediate vicinity of Aβ plaques (Figure 4), they constitute evidence that the Aβ-induced oxidative lipid damage previously reported in vitro[39,40,43] also occurs in vivo.

Various ARA oxidation products are also produced enzymatically, and the activities of enzymes involved in ARA metabolism are indeed increased in the brains of human AD patients.[53−55] Experiments with suitable cyclooxygenase and lipoxygenase inhibitors may define the extent to which the various products we observe to be increased are produced enzymatically. At this point, however, there are no enzymatic processes believed to be involved in HNE production and therefore, we postulate that free-radical-mediated processes are responsible for the aberrantly high levels of ARA-derived species in our experiments. Given that at least some lipid oxidation products have both neurotoxic and fibrillogenic potential, these results have several implications.

One implication is that the presumed neurotoxicity of Aβ peptides in AD may be an indirect effect, mediated not by direct action of Aβ peptides on cells, but rather by their ability to convert PUFAs into neurotoxic products. Others have suggested that PUFA degradation products are neurotoxic in AD, but their origin has not been linked to Aβ peptides.[14−18,23,56] The mechanism by which Aβ peptides promote oxidative PUFA degradation involves the high affinity binding of copper ions by Aβ peptides and redox cycling.[1,39−43,57,58] When operating on ARA, this mechanism yields a mixed array of eicosanoid stereoisomers, some of which are elevated in AD.[44,45,59−61] It also yields smaller neurotoxic molecules such as hydroxyalkenals, acrolein, and malondialdehyde[62−67] that distribute in human brain in the same pattern we observe for increased ARA degradation in mice.[17] In addition to accumulating, they may also covalently modify proteins, alter glial cell function,[68,69] or induce an inflammatory response, one or more of which may cause the kind of slowly progressive neuronal loss that is characteristic of AD.[63,64]

A second implication of our results is that amyloid plaque formation may also be a consequence of Aβ-induced oxidative ARA degradation. ARA is an omega-6 PUFA, which characteristically yields HNE upon oxidative degradation.[13] HNE is potently fibrillogenic, and reduces the concentration at which Aβ40 spontaneously forms fibrils by several orders of magnitude.[39,40,43,70] In other words, nonfibrillar Aβ promotes its own aggregation into fibrils in the presence of copper and omega-6 PUFAs.[1] Therefore, the same general mechanism giving rise to neurotoxic degradation products as described above, may also account for fibril formation in AD. In this scenario, fibril formation would be a byproduct rather than the main cause of the disease, and may even serve a protective role by preventing the formation of redox-active Aβ-copper complexes.[71] DHA, another prevalent PUFA in the brain, yields some of the same neurotoxic products as omega-6 PUFAs when subjected to oxidative degradation, except that HHE is produced instead of HNE.[72] HHE and HNE are both neurotoxic,[73] but HHE does not promote fibril formation in vitro.[43] Therefore, the oxidative degradation of DHA may result in neurotoxicity without fibril formation, and the differential production of HNE from ARA, versus HHE from DHA, may explain the sometimes poor correlation observed between plaque burden and neuronal loss in human AD.[74,75]

A third implication is that the pathogenesis of AD may not depend solely on the local abundance of Aβ peptides in a particular tissue compartment, but also on the abundance of other compounds that react with Aβ peptides or that counteract its prooxidant properties. For example, the relative abundance of omega-3 and omega-6 PUFAs may determine whether or not plaques form in response to oxidative stress. Strategies to alter their concentrations in the brain have shown promising effects on plaque formation in animal models,[76−78] but their effects on neurotoxicity are not yet clear. Aβ-induced oxidative PUFA degradation also depends on the availability of both a redox-active metal ion such as copper, and an electron donor with a high reduction potential, such as ascorbate. The in vivo antioxidant activity of any given compound is difficult to gauge and ascorbate, which is widely regarded as an antioxidant, may be highly prooxidant in the presence of Cu(II).[39,40,57] Assuming that Aβ peptides are necessary for AD pathogenesis, but that other factors determine the severity of disease or plaque burden, therapy aimed at preventing oxidative lipid damage may be as effective for AD therapy as reducing Aβ protein levels.

The most abundant antioxidant in many tissues, glutathione, is effective at neutralizing lipid-derived neurotoxins such as hydroxyalkenals, acrolein, and malondialdehyde.[19,79−84] It may, therefore, neutralize the toxic products of PUFA oxidation, while a deficiency may leave various toxic mechanisms unopposed.[68,85] The key functional group in glutathione is a free sulfhydryl group, which is noteworthy because the incidence of AD is inversely correlated with the number of cysteine residues bearing free sulfhydryl groups in apoE.[86−88] Within a lipoprotein particle, these cysteine side chains are in close proximity to fatty acyl chains, and present at a high concentration relative to those chains and other antioxidant compounds. The presence of even a single sulfhydryl group offers significant antioxidant[89] and neurotoxin-neutralizing potential,[90] so the risk of developing AD with different apoE isoforms may be due to differences in their ability to neutralize neurotoxic PUFA oxidation products.

Beyond these implications, the results presented herein are noteworthy for providing evidence that Aβ-associated oxidative PUFA degradation operates in both mouse models and human AD brain. Moreover, this mechanism appears to be less active in mouse cerebellum, just as the cerebellum is largely spared in human AD. The TG mice used in this study are models of what is essentially familial AD, so it is often unclear whether or not they yield information that is relevant to sporadic human AD. Therefore, it is significant that a product of PUFA oxidation, namely, HNE, which is known to be produced by Aβ-copper complexes in vitro by process that we have now shown to be

DOI: 10.1021/acschemneuro.5b00316
ACS Chem. Neurosci. 2016, 7, 367−377

accelerated in vivo, is found in close association with amyloid plaques in both mouse models and in human AD.

It is also noteworthy that similar results were obtained from two mouse models that differed substantially in their genetic structure, and in the age at which histopathology develops. The data indicates that ARA degradation occurs to a greater extent in the hippocampus of 5xFAD compared to J20 mice (Figure 2d vs Figure 3d). This observation is consistent with the earlier development of histopathology in the 5xFAD model.

HNE-modified proteins in both mouse models and human tissue are found in the vicinity of plaques, but not actually in plaques. The absence of HNE-modified proteins in a plaque could have a trivial explanation such as blocking by anti-Aβ antibodies. Alternatively, and more intriguingly, their absence in plaques may indicate that Aβ fibrils/plaques are surrounded by another physical form of Aβ, one that is redox active and that leads to neurotoxic lipid oxidation products. If true, it remains unclear whether fibrils are a detoxified form of Aβ,[71] or whether fibrillar Aβ is in equilibrium with a redox-active toxic form of Aβ. Yet another possibility is that amyloid plaques are centers of redox activity and oxidative stress. Redox active metal ions are known to accumulate in amyloid plaques,[58] and any HNE produced by the action of these ions on omega-6 PUFAs may have been responsible for inducing Aβ fibrillization and plaque formation. However, the HNE produced may also diffuse and create HNE-modified proteins other than Aβ in the vicinity of the plaque.

An important caveat to this work is that ICV injection does not deliver radiolabeled ARA to the brain in the same manner as ARA derived from the diet. Therefore, its distribution and vulnerability to oxidative degradation may differ from naturally occurring ARA. Delivering ^{14}C-ARA, or even ^{13}C-ARA through the diet or via IV injection is not feasible at this time because the vast majority of labeled material will be intercepted by the liver, and possibly processed into different materials that ultimately reach the brain and confound our results. Indeed, DeGeorge et al. showed that only 0.2% of IV injected 1-[^{14}C]-ARA reached the brain; out of which close to 20% consisted of aqueous-soluble radioactive metabolites.[91] In contrast, PUFAs delivered by ICV injection are largely retained in the brain.[50,92,93]

In Conclusion. Exogenously introduced ARA has been shown to enter a cellular pool that undergoes accelerated conversion to polar degradation products in the immediate vicinity of Aβ plaques, in both mouse models of AD, and human cases of AD. The mechanism may involve Aβ-induced Cu-mediated oxidative ARA degradation as previously observed in vitro, and further investigation of its therapeutic implications is warranted. Because the products of oxidative ARA degradation are both neurotoxic and fibrillogenic, this mechanism has the potential to explain both the neuronal loss, and the formation of amyloid plaques in AD. It also has the potential to explain other key features of AD, such as the poor correlation between plaque burden and disease severity, and the strong correlation between disease incidence and apoE isoforms.

METHODS

Reagents. Unlabeled ARA was purchased from Nu-Check Prep Inc. (Elysian, MN). [1-^{14}C]-ARA was purchased from Moravek Biochemicals (Brea, Ca). [U-^{14}C]-ARA was obtained by special order from PerkinElmer (Waltham, MA). All other chemicals were purchased from Fisher Scientific (Pittsburgh, PA).

Animals. Mice were obtained from The Jackson Laboratory (Bar Harbor, ME). B6SJL (5XFAD) mice express human amyloid precursor protein with the Swedish (K670N, M671L), Florida (I716V), and London (V717I) mutations, and human presenilin 1 with the M146L and L286V mutations. Expression of both transgenes is regulated by a Thy1 promoter, and amyloid plaques begin appearing in the brains by 2 months of age. Age matched B6SJLF1/J mice were used as wild-type (WT) controls. B6.Cg-Tg (J20) mice express human APP with the Swedish (K670N/M671L) and the Indiana (V717F) mutations. Expression of this transgene is regulated by a platelet-derived growth factor beta (PDGFB) promoter, and amyloid plaques begin appearing in the brains by 10 months of age. Age matched C57BL/6J mice, were used as WT controls. All mice used in these experiments were 16−21 months old, and the majority of plaques were confined to the hippocampus and entorhinal cortex. All experimental procedures and animal care were in compliance with the National Institutes of Health (NIH) guidelines for the Care and Use of Laboratory Animals.

Intracerebroventricular (ICV) Injection. An aliquot of either [U-^{14}C]-ARA or [1-^{14}C]-ARA in ethanol was dried under argon in polytetrafluoroethylene tubes and resuspended in PBS with 10% DMSO. ICV injection was performed under isoflurane anesthesia. Volumes of 4−8 μL (0.2−0.4 μCi) were injected 0.35 mm posterior to bregma, 1 mm right of the midline and 2 mm below the subarachnoid surface at a rate of 2 μL/min via 33 gauge needle. Postoperative pain was alleviated by subcutaneous injection of Loxicam (Norbrook, Newry, North Ireland). Animals were monitored for 72 h and then euthanized using carbon dioxide. The ARA stock purity was tested periodically using chromatographic analysis on a reverse phase column (as described below). A slow decrease in ARA purity with a concomitant increase in the prevalence of oxidation derivatives was observed when the stock was kept in PBS + 10% DMSO for more than a week at −80 °C. Therefore, the ARA stock was kept in ethanol until no earlier than 3 days before the ICV injection when it was resuspended in PBS + 10% DMSO. Only stock with >95% purity was used for injections.

Whole brains were removed and frozen on dry ice within 3 min postmortem. Comparable sized tissues from the hippocampus (including dentate gyrus) and cerebellum were dissected and transferred to high-recovery clear borosilicate glass autosampler vials for weighing (9512S, Microsolv Technology Corp., Eatontown, NJ). The mass of the dissected tissue samples ranged from 10 to 40 mg. Tissue processing was done immediately after dissection. The remaining brain tissue (brain minus cerebellum and hippocampus) was also transferred to autosampler vials for weighing (mass range 300−340 mg). Histopathological examination of brain tissue after ICV injection of the materials described above showed minimal architectural disruption near the injection site, and none away from the site. There was no evidence of inflammatory response near the injection site, in the ventricular ependymal, or elsewhere in the brain (data not shown).

Lipid Extraction and Saponification. Extraction was performed using a modified Bligh−Dyer (BD) procedure (Axelsen and Murphy, JLR 2010). Briefly, tissues from the cerebellum and hippocampus were sonicated with a tip sonicator for 60 s in 760 μL of monophase (400 μL of methanol, 200 μL of dichloromethane, and 160 μL of 5 mM ammonium chloride). The homogenate was transferred to a 15 mL glass tube (Fisher Scientific, Pittsburgh, PA) where a mixture of 760 μL of monophase, 200 μL of dichloromethane, and 160 μL of water were added for each 5 mg tissue, and the tube was vortexed. The three resulting phases were separated by 1 min of low speed centrifugation. The lower (dichloromethane) phase (~1−2 mL) was withdrawn, transferred to a new glass tube, and dried under argon. The remaining brain tissue (brain minus cerebellum and hippocampus) was homogenized in 800 μL of water. Then 200 μL of this homogenate was transferred to a fresh tube and processed as described above.

Saponification was performed by resuspending the residue from the lower, dichloromethane phase of the BD extraction in 85% MeOH in water with 0.5 M NH_4OH (2 mL final volume), and incubating at 80 °C for 1 h. Following saponification, samples were cooled to room temperature, acidified with 100 μL of 5 M HCl, and extracted four

DOI: 10.1021/acschemneuro.5b00316
ACS Chem. Neurosci. 2016, 7, 367−377

times with 1 mL of isooctane. The isooctane was evaporated under argon, and the residue were dissolved in 150 μL of ethanol for analysis by high performance liquid chromatography (HPLC).

HPLC and Mass Spectrometry Analyses. Saponified samples in ETOH (20 μL) were separated by HPLC using a 4.6 × 150 mm C18 column (XDB-C18, Agilent, Santa Clara, CA) and a mixed binary mobile phase pumped at 0.35 mL/min. Solvent A was 60% acetonitrile, 40% H_2O, and 0.1% formic acid; solvent B was 100% acetonitrile and 0.1% formic acid. Upon sample injection, the mobile phase was changed linearly from 30% to 100% B over 55 min and held at 100% B for 9 min. Before injecting each sample, the column was equilibrated with 30% B for 15 min. Column performance under these conditions was characterized by analyzing nonradioactive samples on an ABI 4000 mass spectrometer (Toronto, Canada) operating in negative ion multiple reaction monitoring (MRM) mode. NH_4OH (0.15 M) in MeOH at 50 μL/min was mixed in prior to the MS analysis to induce the fatty acids negative charge. The DP was −75 V, CAD was 7 psi, CE was −20 V, the IS was −4500 V, and the nitrogen drying gas temperature was 300 °C. Fractions between 0 and 60 min were collected and counted for radioactivity. Radioactivity in each fraction was divided by the total radioactivity collected from the column to obtain the prevalence of each and data from 6−10 mice was averaged.

Specific Radioactivity Determinations. Radioactive samples were mixed with 4 mL of ECOLITE scintillation fluid (MP biomedicals, Santa Ana CA) in 5 mL scintillation vials (Lake Charles, Lake Charles LA) and counted for 1 min in LS 6500 Multipurpose Scintillation Counter (Beckman Coulter, Brea, CA) operating in auto-DPM mode (all results are reported in disintegrations-per-minute, DPM). The activities in an aliquot of the lower dicholoromethane phase of a Bligh−Dyer extract (BD_L) and in a suspension of the upper and middle phases (BD_{MU}) were measured, scaled by the volume of each phase (V_L and V_{MU}), summed, and divided by the mass of the tissue sample (M_t) to obtain its specific radioactivity (eq 1). Approximately 1/10 of the injections yielded a dramatically high specific radioactivity in the hippocampus (more than twice the average); these abnormalities were attributed to inadvertent injection directly into the hippocampus and were excluded from the analysis. To correct for differences in the amount of radioactivity injected into each animal, the specific radioactivities in the cerebellum and hippocampus were divided by the specific radioactivity of the total brain to obtain relative specific radioactivities (eq 2).

$$(BD_L V_L + BD_{MU} V_{MU})/M_t = SA \quad (1)$$

$$SA_{region}/SA_{whole\_brain} = \text{relative specific activity}_{region} \quad (2)$$

Immunohistopathology. Anti-Aβ murine monoclonal antibody 6E10 was purchased from Covance (Princeton, NJ). Rabbit anti-4-hydroxy-2-nonenal-His polyclonal antibody (HNE11-S) was obtained from Genox Corporation (Baltimore, MD). Fluorescent secondary antibodies were goat anti-mouse Alexa Fluor Red 594 and goat anti-rabbit Oregon Green 488 and obtained from Invitrogen (Grand Island, NY). Paraffin embedded paraformaldehyde fixed sections of AD hippocampus were obtained from the brain bank at Case Western Reserve University. Slides were deparaffinized by two immersions in xylenes for 5 min each, followed by rehydration through decreasing concentrations of ethanol (100%, 95%, 80%, and 70%) for 1 min each and finally ending in water. Primary antibodies were diluted 1:200, applied to the tissue slices, and incubated overnight at 4 °C in a humidified chamber. After rinsing, secondary antibodies were applied to the tissue slices and incubated overnight at 4 °C.

■ ASSOCIATED CONTENT

Supporting Information

The Supporting Information is available free of charge on the ACS Publications website at DOI: 10.1021/acschemneuro.5b00316.

Table of MRM transitions and stained tissue sections (PDF)

■ AUTHOR INFORMATION

Corresponding Author

*Tel: 215-898-5000. E-mail: axe@pharm.med.upenn.edu.

Author Contributions

P.H.A., I.V.J.M., and R.F. designed the experiments, wrote the paper, and approved the final manuscript. R.F., H.E.S., J.L., and Y.G. performed the experiments.

Funding

This work was supported by NS74178 and GM76201 from the NIH, and grants from the Alzheimer's Association, the American Health Assistance Foundation, and the Glenn Foundation (all to P.H.A.).

Notes

The authors declare no competing financial interest.

■ REFERENCES

(1) Axelsen, P. H., Komatsu, H., and Murray, I. V. J. (2011) Oxidative Stress and Cell Membranes in the Pathogenesis of Alzheimer's Disease. *Physiology 26*, 54−69.

(2) Butterfield, D. A., and Boyd-Kimball, D. (2004) Amyloid Beta-Peptide(1−42) Contributes to the Oxidative Stress and Neurodegeneration Found in Alzheimer Disease Brain. *Brain Pathol. 14*, 426−432.

(3) Pratico, D., and Delanty, N. (2000) Oxidative Injury in Diseases of the Central Nervous System: Focus on Alzheimer's Disease. *Am. J. Med. 109*, 577−585.

(4) Butterfield, D. A., and Lauderback, C. M. (2002) Lipid Peroxidation and Protein Oxidation in Alzheimer's Disease Brain: Potential Causes and Consequences Involving Amyloid Beta-Peptide-Associated Free Radical Oxidative Stress. *Free Radical Biol. Med. 32*, 1050−1060.

(5) Markesbery, W. R. (1999) The Role of Oxidative Stress in Alzheimer Disease. *Arch. Neurol. 56*, 1449−1452.

(6) Atwood, C. S., Huang, X. D., Khatri, A., Scarpa, R. C., Kim, Y. S., Moir, R. D., Tanzi, R. E., Roher, A. E., and Bush, A. I. (2000) Copper Catalyzed Oxidation of Alzheimer A Beta. *Cell. Mol. Biol. 46*, 777−783.

(7) Atwood, C. S., Huang, X. D., Moir, R. D., Tanzi, R. E., and Bush, A. I. (1999) Role of Free Radicals and Metal Ions in the Pathogenesis of Alzheimer's Disease. *Met. Ions Biol. Syst. 36*, 309−364.

(8) Liu, J. J., Green, P., John Mann, J., Rapoport, S. I., and Sublette, M. E. (2015) Pathways of Polyunsaturated Fatty Acid Utilization: Implications for Brain Function in Neuropsychiatric Health and Disease. *Brain Res. 1597*, 220−246.

(9) Bazinet, R. P., and Laye, S. (2014) Polyunsaturated Fatty Acids and Their Metabolites in Brain Function and Disease. *Nat. Rev. Neurosci. 15*, 771−785.

(10) Schneider, C., Tallman, K. A., Porter, N. A., and Brash, A. R. (2001) Two Distinct Pathways of Formation of 4-Hydroxynonenal - Mechanisms of Nonenzymatic Transformation of the 9-and 13-Hydroperoxides of Linoleic Acid to 4-Hydroxyalkenals. *J. Biol. Chem. 276*, 20831−20838.

(11) Arlt, S., Beisiegel, U., and Kontush, A. (2002) Lipid Peroxidation in Neurodegeneration: New Insights into Alzheimer's Disease. *Curr. Opin. Lipidol. 13*, 289−294.

(12) Schneider, C., Porter, N. A., and Brash, A. R. (2008) Routes to 4-Hydroxynonenal: Fundamental Issues in the Mechanisms of Lipid Peroxidation. *J. Biol. Chem. 283*, 15539−15543.

(13) Uchida, K. (2003) 4-Hydroxy-2-Nonenal: a Product and Mediator of Oxidative Stress. *Prog. Lipid Res. 42*, 318−343.

(14) Montine, T. J., Neely, M. D., Quinn, J. F., Beal, M. F., Markesbery, W. R., Roberts, L. J., and Morrow, J. D. (2002) Lipid Peroxidation in Aging Brain and Alzheimer's Disease. *Free Radical Biol. Med. 33*, 620−626.

DOI: 10.1021/acschemneuro.5b00316
ACS Chem. Neurosci. 2016, 7, 367−377

(15) Lovell, M. A., Ehmann, W. D., Mattson, M. P., and Markesbery, W. R. (1997) Elevated 4-Hydroxynonenal in Ventricular Fluid in Alzheimer's Disease. *Neurobiol. Aging 18*, 457−461.
(16) Markesbery, W. R., and Lovell, M. A. (1998) Four-Hydroxynonenal, a Product of Lipid Peroxidation, Is Increased in the Brain in Alzheimer's Disease. *Neurobiol. Aging 19*, 33−36.
(17) Williams, T. I., Lynn, B. C., Markesbery, W. R., and Lovell, M. A. (2006) Increased Levels of 4-Hydroxynonenal and Acrolein, Neurotoxic Markers of Lipid Peroxidation, in the Brain in Mild Cognitive Impairment and Early Alzheimer's Disease. *Neurobiol. Aging 27*, 1094−1099.
(18) Mark, R. J., Lovell, M. A., Markesbery, W. R., Uchida, K., and Mattson, M. P. (1997) A Role for 4-Hydroxynonenal, an Aldehydic Product of Lipid Peroxidation, in Disruption of Ion Homeostasis and Neuronal Death Induced by Amyloid Beta-Peptide. *J. Neurochem. 68*, 255−264.
(19) Kruman, I., BruceKeller, A. J., Bredesen, D., Waeg, G., and Mattson, M. P. (1997) Evidence That 4-Hydroxynonenal Mediates Oxidative Stress-Induced Neuronal Apoptosis. *J. Neurosci. 17*, 5089−5100.
(20) Keller, J. N., Pang, Z., Geddes, J. W., Begley, J. G., Germeyer, A., Waeg, G., and Mattson, M. P. (1997) Impairment of Glucose and Glutamate Transport and Induction of Mitochondrial Oxidative Stress and Dysfunction in Synaptosomes by Amyloid Beta-Peptide: Role of the Lipid Peroxidation Product 4-Hydroxynonenal. *J. Neurochem. 69*, 273−284.
(21) Lovell, M. A., Xie, C. S., and Markesbery, W. R. (2001) Acrolein Is Increased in Alzheimer's Disease Brain and Is Toxic to Primary Hippocampal Cultures. *Neurobiol. Aging 22*, 187−194.
(22) Montine, K. S., Kim, P. J., Olson, S. J., Markesbery, W. R., and Montine, T. J. (1997) 4-Hydroxy-2-Nonenal Pyrrole Adducts in Human Neurodegenerative Disease. *J. Neuropathol. Exp. Neurol. 56*, 866−871.
(23) Montine, K. S., Olson, V. J., Amarnath, V., Whetsell, W. O., Jr., Graham, D. G., and Montine, T. J. (1997) Immunohistochemical Detection of 4-Hydroxy-2-Nonenal Adducts in Alzheimer's Disease Is Associated With Inheritance of APOE4. *Am. J. Pathol. 150*, 437−443.
(24) Sayre, L. M., Zelasko, D. A., Harris, P. L. R., Perry, G., Salomon, R. G., and Smith, M. A. (1997) 4-Hydroxynonenal-Derived Advanced Lipid Peroxidation End Products Are Increased in Alzheimer's Disease. *J. Neurochem. 68*, 2092−2097.
(25) Smith, M. A., Hirai, K., Hsiao, K., Pappolla, M. A., Harris, P. L. R., Siedlak, S. L., Tabaton, M., and Perry, G. (1998) Amyloid-Beta Deposition in Alzheimer Transgenic Mice Is Associated With Oxidative Stress. *J. Neurochem. 70*, 2212−2215.
(26) Takeda, A., Smith, M. A., Avila, J., Nunomura, A., Siedlak, S. L., Zhu, X. W., Perry, G., and Sayre, L. M. (2000) In Alzheimer's Disease, Heme Oxygenase Is Coincident With Alz50, an Epitope of Tau Induced by 4-Hydroxy-2-Nonenal Modification. *J. Neurochem. 75*, 1234−1241.
(27) Wataya, T., Nunomura, A., Smith, M. A., Siedlak, S. L., Harris, P. L. R., Shimohama, S., Szweda, L. I., Kaminski, M. A., Avila, J., Price, D. L., Cleveland, D. W., Sayre, L. M., and Perry, G. (2002) High Molecular Weight Neurofilament Proteins Are Physiological Substrates of Adduction by the Lipid Peroxidation Product Hydroxynonenal. *J. Biol. Chem. 277*, 4644.
(28) Mucke, L., Masliah, E., Yu, G. Q., Mallory, M., Rockenstein, E. M., Tatsuno, G., Hu, K., Kholodenko, D., Johnson-Wood, K., and McConlogue, L. (2000) High-Level Neuronal Expression of A Beta(1−42) in Wild-Type Human Amyloid Protein Precursor Transgenic Mice: Synaptotoxicity Without Plaque Formation. *J. Neurosci. 20*, 4050−4058.
(29) Kamenetz, F., Tomita, T., Hsieh, H., Seabrook, G., Borchelt, D., Iwatsubo, T., Sisodia, S., and Malinow, R. (2003) APP Processing and Synaptic Function. *Neuron 37*, 925−937.
(30) Ting, J. T., Kelley, B. G., Lambert, T. J., Cook, D. G., and Sullivan, J. M. (2007) Amyloid Precursor Protein Overexpression Depresses Excitatory Transmission Through Both Presynaptic and Postsynaptic Mechanisms. *Proc. Natl. Acad. Sci. U. S. A. 104*, 353−358.
(31) Selkoe, D. J. (2008) Soluble Oligomers of the Amyloid Beta-Protein Impair Synaptic Plasticity and Behavior. *Behav. Brain Res. 192*, 106−113.
(32) Shankar, G. M., Li, S. M., Mehta, T. H., Garcia-Munoz, A., Shepardson, N. E., Smith, I., Brett, F. M., Farrell, M. A., Rowan, M. J., Lemere, C. A., Regan, C. M., Walsh, D. M., Sabatini, B. L., and Selkoe, D. J. (2008) Amyloid-Beta Protein Dimers Isolated Directly From Alzheimer's Brains Impair Synaptic Plasticity and Memory. *Nat. Med. 14*, 837−842.
(33) Deshpande, A., Kawai, H., Metherate, R., Glabe, C. G., and Busciglio, J. (2009) A Role for Synaptic Zinc in Activity-Dependent A Beta Oligomer Formation and Accumulation at Excitatory Synapses. *J. Neurosci. 29*, 4004−4015.
(34) Koffie, R. M., Meyer-Luehmann, M., Hashimoto, T., Adams, K. W., Mielke, M. L., Garcia-Alloza, M., Micheva, K. D., Smith, S. J., Kim, M. L., Lee, V. M., Hyman, B. T., and Spires-Jones, T. L. (2009) Oligomeric Amyloid β Associates With Postsynaptic Densities and Correlates With Excitatory Synapse Loss Near Senile Plaques. *Proc. Natl. Acad. Sci. U. S. A. 106*, 4012.
(35) Dinamarca, M. C., Weinstein, D., Monasterio, O., and Inestrosa, N. C. (2011) The Synaptic Protein Neuroligin-1 Interacts With the Amyloid B-Peptide. Is There a Role in Alzheimer's Disease? *Biochemistry 50*, 8127−8137.
(36) D'Amelio, M., and Rossini, P. M. (2012) Brain Excitability and Connectivity of Neuronal Assemblies in Alzheimer's Disease: From Animal Models to Human Findings. *Prog. Neurobiol. 99*, 42−60.
(37) Hartter, D. E., and Barnea, A. (1988) Evidence for Release of Copper in the Brain - Depolarization-Induced Release of Newly Taken-Up Copper-67. *Synapse 2*, 412−415.
(38) Kardos, J., Kovacs, I., Hajos, F., Kalman, M., and Simonyi, M. (1989) Nerve-Endings From Rat-Brain Tissue Release Copper Upon Depolarization - A Possible Role in Regulating Neuronal Excitability. *Neurosci. Lett. 103*, 139−144.
(39) Murray, I. V. J., Sindoni, M. E., and Axelsen, P. H. (2005) Promotion of Oxidative Lipid Membrane Damage by Amyloid Beta Proteins. *Biochemistry 44*, 12606−12613.
(40) Murray, I. V. J., Liu, L., Komatsu, H., Uryu, K., Xiao, G., Lawson, J. A., and Axelsen, P. H. (2007) Membrane Mediated Amyloidogenesis and the Promotion of Oxidative Lipid Damage by Amyloid Beta Proteins. *J. Biol. Chem. 282*, 9335−9345.
(41) Koppaka, V., and Axelsen, P. H. (2000) Accelerated Accumulation of Amyloid Beta Proteins on Oxidatively Damaged Lipid Membranes. *Biochemistry 39*, 10011−10016.
(42) Koppaka, V., Paul, C., Murray, I. V. J., and Axelsen, P. H. (2003) Early Synergy Between Aβ42 and Oxidatively Damaged Membranes in Promoting Amyloid Fibril Formation by Aβ40. *J. Biol. Chem. 278*, 36277−36284.
(43) Liu, L., Komatsu, H., Murray, I. V. J., and Axelsen, P. H. (2008) Promotion of Amyloid β Protein Misfolding and Fibrillogenesis by a Lipid Oxidation Product. *J. Mol. Biol. 377*, 1236−1250.
(44) Pratico, D., Lee, V. M. Y., Trojanowski, J. Q., Rokach, J., and FitzGerald, G. A. (1998) Increased F-2-Isoprostanes in Alzheimer's Disease: Evidence for Enhanced Lipid Peroxidation in Vivo. *FASEB J. 12*, 1777−1783.
(45) Pratico, D., Clark, C. M., Lee, V. M. Y., Trojanowski, J. Q., Rokach, J., and FitzGerald, G. A. (2000) Increased 8,12-Iso-IPF(2 Alpha)-VI in Alzheimer's Disease: Correlation of a Noninvasive Index of Lipid Peroxidation With Disease Severity. *Ann. Neurol. 48*, 809−812.
(46) Magni, F., Galbusera, C., Tremolada, L., Ferrarese, C., and Kienle, M. G. (2002) Characterisation of Adducts of the Lipid Peroxidation Product 4-Hydroxy-2-Nonenal and Amyloid Beta-Peptides by Liquid Chromatography/Electrospray Ionisation Mass Spectrometry. *Rapid Commun. Mass Spectrom. 16*, 1485−1493.
(47) Ando, Y., Brannstrom, T., Uchida, K., Nyhlin, N., Nasman, B., Suhr, O., Yamashita, T., Olsson, T., El Salhy, M., Uchino, M., and Ando, M. (1998) Histochemical Detection of 4-Hydroxynonenal Protein in Alzheimer Amyloid. *J. Neurol. Sci. 156*, 172−176.

DOI: 10.1021/acschemneuro.5b00316
ACS Chem. Neurosci. 2016, 7, 367−377

(48) Rofina, J. E., Singh, K., Skoumalova-Vesela, A., van Ederen, A. M., van Asten, A. J. A. M., Wilhelm, J., and Gruys, E. (2004) Histochemical Accumulation of Oxidative Damage Products Is Associated With Alzheimer-Like Pathology in the Canine. *Amyloid 11*, 90−100.
(49) Ellis, G., Fang, E., Maheshwari, M., Roltsch, E., Holcomb, L., Zimmer, D., Martinez, D., and Murray, I. V. J. (2010) Lipid Oxidation and Modification of Amyloid-Beta (A Beta) in Vitro and in Vivo. *J. Alzheimer's Dis. 22*, 593−607.
(50) DeMar, J. C., Ma, K. Z., Bell, J. M., and Rapoport, S. I. (2004) Half-Lives of Docosahexaenoic Acid in Rat Brain Phospholipids Are Prolonged by 15 Weeks of Nutritional Deprivation of N-3 Polyunsaturated Fatty Acids. *J. Neurochem. 91*, 1125−1137.
(51) Shaw, G. G. (1974) Some Shortcomings of Direct Intraventricular-Injection in Mice. *Br. J. Pharmacol. 50*, 603−605.
(52) Mims, C. A. (1960) Intracerebral Injections and the Growth of Viruses in the Mouse Brain. *Br. J. Exp. Pathol. 41*, 52.
(53) Boutaud, O., Andreasson, K. I., Zagol-Ikapitte, I., and Oates, J. (2005) Cyclooxygenase-Dependent Lipid-Modification of Brain Proteins. *Brain Pathol. 15*, 139−142.
(54) Zagol-Ikapitte, I., Masterson, T. S., Amarnath, V., Montine, T. J., Andreasson, K. I., Boutaud, O., and Oates, J. A. (2005) Prostaglandin H-2-Derived Adducts of Proteins Correlate With Alzheimer's Disease Severity. *J. Neurochem. 94*, 1140−1145.
(55) Rao, J. S., Rapoport, S. I., and Kim, H. W. (2011) Altered Neuroinflammatory, Arachidonic Acid Cascade and Synaptic Markers in Postmortem Alzheimer's Disease Brain. *Transl. Psychiatry 1*, e31.
(56) Bassett, C. N., Neely, M. D., Sidell, K. R., Markesbery, W. R., Switt, L. L., and Montine, T. J. (1999) Cerebrospinal Fluid Lipoproteins Are More Vulnerable to Oxidation in Alzheimer's Disease and Are Neurotoxic When Oxidized Ex Vivo. *Lipids 34*, 1273−1280.
(57) Komatsu, H., Liu, L., Murray, I. V., and Axelsen, P. H. (2007) A Mechanistic Link Between Oxidative Stress and Membrane Mediated Amyloidogenesis Revealed by Infrared Spectroscopy. *Biochim. Biophys. Acta, Biomembr. 1768*, 1913−1922.
(58) Eskici, G., and Axelsen, P. H. (2012) Copper and Oxidative Stress in the Pathogenesis of Alzheimer's Disease. *Biochemistry 51*, 6289−6311.
(59) Pratico, D., Uryu, K., Leight, S., Trojanowswki, J. Q., and Lee, V. M. Y. (2001) Increased Lipid Peroxidation Precedes Amyloid Plaque Formation in an Animal Model of Alzheimer Amyloidosis. *J. Neurosci. 21*, 4183−4187.
(60) Yao, Y., Zhukareva, V., Sung, S., Clark, C. M., Rokach, J., Lee, V. M. Y., Trojanowski, J. Q., and Pratico, D. (2003) Enhanced Brain Levels of 8,12-Iso-IPF(2 Alpha)-VI Differentiate AD From Frontotemporal Dementia. *Neurology 61*, 475−478.
(61) Pratico, D. (2010) The Neurobiology of Isoprostanes and Alzheimer's Disease. *Biochim. Biophys. Acta, Mol. Cell Biol. Lipids 1801*, 930−933.
(62) Ozcankaya, R., and Delibas, N. (2002) Malondialdehyde, Superoxide Dismutase, Melatonin, Iron, Copper, and Zinc Blood Concentrations in Patients With Alzheimer Disease: Cross-Sectional Study. *Croat. Med. J. 43*, 28−32.
(63) Bai, J., and Mei, Y. (2011) Overexpression of Aldehyde Dehydrogenase-2 Attenuates Neurotoxicity Induced by 4-Hydroxynonenal in Cultured Primary Hippocampal Neurons. *Neurotoxic. Res. 19*, 412−422.
(64) Huang, Y. J., Jin, M. H., Pi, R. B., Zhang, J. J., Ouyang, Y., Chao, X. J., Chen, M. H., Liu, P. Q., Yu, J. C., Ramassamy, C., Dou, J., Chen, X. H., Jiang, Y. M., and Qin, J. (2013) Acrolein Induces Alzheimer's Disease-Like Pathologies in Vitro and in Vivo. *Toxicol. Lett. 217*, 184−191.
(65) Hayashi, T., Shishido, N., Nakayama, K., Nunomura, A., Smith, M. A., Perry, G., and Nakamura, M. (2007) Lipid Peroxidation and 4-Hydroxy-2-Nonenal Formation by Copper Ion Bound to Amyloid-Beta Peptide. *Free Radical Biol. Med. 43*, 1552−1559.
(66) Awasthi, Y. C., Sharma, R., Cheng, J. Z., Yang, Y., Sharma, A., Singhal, S. S., and Awasthi, S. (2003) Role of 4-Hydroxynonenal in Stress-Mediated Apoptosis Signaling. *Mol. Aspects Med. 24*, 219−230.
(67) Liu, Q., Raina, A. K., Smith, M. A., Sayre, L. M., and Perry, G. (2003) Hydroxynonenal, Toxic Carbonyls, and Alzheimer Disease. *Mol. Aspects Med. 24*, 305−313.
(68) Abramov, A. Y., Canevari, L., and Duchen, M. R. (2003) Changes in Intracellular Calcium and Glutathione in Astrocytes As the Primary Mechanism of Amyloid Neurotoxicity. *J. Neurosci. 23*, 5088−5095.
(69) Miller, V. M., Lawrence, D. A., Mondal, T. K., and Seegal, R. F. (2009) Reduced Glutathione Is Highly Expressed in White Matter and Neurons in the Unperturbed Mouse Brain - Implications for Oxidative Stress Associated With Neurodegeneration. *Brain Res. 1276*, 22−30.
(70) Chen, K., Maley, J., and Yu, P. H. (2006) Potential Implications of Endogenous Aldehydes in Beta-Amyloid Misfolding, Oligomerization and Fibrillogenesis. *J. Neurochem. 99*, 1413−1424.
(71) Cuajungco, M. P., Goldstein, L. E., Nunomura, A., Smith, M. A., Lim, J. T., Atwood, C. S., Huang, X., Farrag, Y. W., Perry, G., and Bush, A. I. (2000) Evidence That the B-Amyloid Plaques of Alzheimer's Disease Represent the Redox-Silencing and Entombment of Abeta by Zinc. *J. Biol. Chem. 275*, 19439−19442.
(72) Long, E. K., Murphy, T. C., Leiphon, L. J., Watt, J., Morrow, J. D., Milne, G. L., Howard, J. R., and Picklo, M. J. (2008) Trans-4-Hydroxy-2-Hexenal Is a Neurotoxic Product of Docosahexaenoic (22:6; N-3) Acid Oxidation. *J. Neurochem. 105*, 714−724.
(73) Long, E. K., and Picklo, M. J. (2010) Trans-4-Hydroxy-2-Hexenal, a Product of N-3 Fatty Acid Peroxidation: Make Some Room HNE. *Free Radical Biol. Med. 49*, 1−8.
(74) Giannakopoulos, P., Herrmann, F. R., Bussiere, T., Bouras, C., Kovari, E., Perl, D. P., Morrison, J. H., Gold, G., and Hof, P. R. (2003) Tangle and Neuron Numbers, but Not Amyloid Load, Predict Cognitive Status in Alzheimer's Disease. *Neurology 60*, 1495−1500.
(75) Nelson, P. T., Jicha, G. A., Schmitt, F. A., Liu, H., Davis, D. G., Mendiondo, M. S., Abner, E. L., and Markesbery, W. R. (2007) Clinicopathologic Correlations in a Large Alzheimer Disease Center Autopsy Cohort: Neuritic Plaques and Neurofibrillary Tangles " Do Count " When Staging Disease Severity. *J. Neuropathol. Exp. Neurol. 66*, 1136−1146.
(76) Sanchez-Mejia, R. O., Newman, J. W., Toh, S., Yu, G. Q., Zhou, Y. U., Halabisky, B., Cisse, M., Scearce-Levie, K., Cheng, I. H., Gan, L., Palop, J. J., Bonventre, J. V., and Mucke, L. (2008) Phospholipase A(2) Reduction Ameliorates Cognitive Deficits in a Mouse Model of Alzheimer's Disease. *Nat. Neurosci. 11*, 1311−1318.
(77) Piro, J. R., Benjamin, D. I., Duerr, J. M., Pi, Y. Q., Gonzales, C., Wood, K. M., Schwartz, J. W., Nomura, D. K., and Samad, T. A. (2012) A Dysregulated Endocannabinoid-Eicosanoid Network Supports Pathogenesis in a Mouse Model of Alzheimer's Disease. *Cell Rep. 1*, 617−623.
(78) Lysenko, L. V., Kim, J., Henry, C., Tyrtyshnaia, A., Kohnz, R. A., Madamba, F., Simon, G. M., Kleschevnikova, N. E., Nomura, D. K., Ezekowitz, R., and Kleschevnikov, A. M. (2014) Monoacylglycerol Lipase Inhibitor JZL184 Improves Behavior and Neural Properties in Ts65Dn Mice, a Model of Down Syndrome. *PLoS One 9*, e114521.
(79) Jeandel, C., Nicolas, M. B., Dubois, F., Nabet-Belleville, F., Penin, F., and Cuny, G. (1989) Lipid Peroxidation and Free Radical Scavengers in Alzheimer's Disease. *Gerontology 35*, 275−282.
(80) Spitz, D. R., Malcolm, R. R., and Roberts, R. J. (1990) Cytotoxicity and Metabolism of 4-Hydroxy-2-Nonenal and 2-Nonenal in H2O2-Resistant Cell-Lines - Do Aldehydic By-Products of Lipid-Peroxidation Contribute to Oxidative Stress. *Biochem. J. 267*, 453−459.
(81) Grune, T., Siems, W. G., Zollner, H., and Esterbauer, H. (1994) Metabolism of 4-Hydroxynonenal, A Cytotoxic Lipid-Peroxidation Product, in Ehrlich Mouse Ascites-Cells at Different Proliferation Stages. *Cancer Res. 54*, 5231−5235.
(82) Ullrich, O., Grune, T., Henke, W., Esterbauer, H., and Siems, W. G. (1994) Identification of Metabolic Pathways of the Lipid-Peroxidation Product 4-Hydroxynonenal by Mitochondria Isolated From Rat-Kidney Cortex. *FEBS Lett. 352*, 84−86.

DOI: 10.1021/acschemneuro.5b00316
ACS Chem. Neurosci. 2016, 7, 367−377

(83) Butterfield, D. A., Pocernich, C. B., and Drake, J. (2002) Elevated Glutathione As a Therapeutic Strategy in Alzheimer's Disease. *Drug Dev. Res. 56*, 428−437.
(84) Chaudhary, P., Sharma, R., Sharma, A., Vatsyayan, R., Yadav, S., Singhal, S. S., Rauniyar, N., Prokai, L., Awasthi, S., and Awasthi, Y. C. (2010) Mechanisms of 4-Hydroxy-2-Nonenal Induced Pro- and Anti-Apoptotic Signaling. *Biochemistry 49*, 6263−6275.
(85) Resende, R., Moreira, P. I., Proenca, T., Deshpande, A., Busciglio, J., Pereira, C., and Oliveira, C. R. (2008) Brain Oxidative Stress in a Triple-Transgenic Mouse Model of Alzheimer Disease. *Free Radical Biol. Med. 44*, 2051−2057.
(86) Khachaturian, A. S., Corcoran, C. D., Mayer, L. S., Zandi, P. P., and Breitner, J. C. S. (2004) Apolipoprotein E Epsilon 4 Count Affects Age at Onset of Alzheimer Disease, but Not Lifetime Susceptibility - The Cache County Study. *Arch. Gen. Psychiatry 61*, 518−524.
(87) Corder, E. H., Saunders, A. M., Strittmatter, W. J., Schmechel, D. E., Gaskell, P. C., Small, G. W., Roses, A. D., Haines, J. L., and Pericakvance, M. A. (1993) Gene Dose of Apolipoprotein-E Type-4 Allele and the Risk of Alzheimers-Disease in Late-Onset Families. *Science 261*, 921−923.
(88) Corder, E. H., Saunders, A. M., Risch, N. J., Strittmatter, W. J., Schmechel, D. E., Gaskell, P. C., Rimmler, J. B., Locke, P. A., Conneally, P. M., Schmader, K. E., Small, G. W., Roses, A. D., Haines, J. L., and Pericakvance, M. A. (1994) Protective Effect of Apolipoprotein-e Type-2 Allele for Late-Onset Alzheimer-Disease. *Nat. Genet. 7*, 180−184.
(89) Bielicki, J. K., and Oda, M. N. (2002) Apolipoprotein A-I-Milano and Apolipoprotein A-I-Paris Exhibit an Antioxidant Activity Distinct From That of Wild-Type Apolipoprotein A-I. *Biochemistry 41*, 2089−2096.
(90) Pedersen, W. A., Chan, S. L., and Mattson, M. P. (2000) A Mechanism for the Neuroprotective Effect of Apolipoprotein E: Isoform-Specific Modification by the Lipid Peroxidation Product 4-Hydroxynonenal. *J. Neurochem. 74*, 1426−1433.
(91) DeGeorge, J. J., Noronha, J. G., Bell, J., Robinson, P., and Rapoport, S. I. (1989) Intravenous-Injection of [1-C-14] Arachidonate to Examine Regional Brain Lipid-Metabolism in Unanesthetized Rats. *J. Neurosci. Res. 24*, 413−423.
(92) Chen, C. T., Liu, Z., and Bazinet, R. P. (2011) Rapid De-Esterification and Loss of Eicosapentaenoic Acid From Rat Brain Phospholipids: an Intracerebroventricular Study. *J. Neurochem. 116*, 363−373.
(93) Lin, L. E., Chen, C. T., Hildebrand, K. D., Liu, Z., Hopperton, K. E., and Bazinet, R. P. (2015) Chronic Dietary N-6 PUFA Deprivation Leads to Conservation of Arachidonic Acid and More Rapid Loss of DHA in Rat Brain Phospholipids. *J. Lipid Res. 56*, 390−402.

DOI: 10.1021/acschemneuro.5b00316
ACS Chem. Neurosci. 2016, 7, 367−377